*American Mineralogist, Volume 82, pages 1198–1209, 1997*

# Experimental study of the system phlogopite-diopside from 3.5 to 17 GPa

**ROBERT W. LUTH**

C.M. Scarfe Laboratory of Experimental Petrology, Department of Earth and Atmospheric Sciences, University of Alberta, Edmonton, Alberta T6G 2E3, Canada

## ABSTRACT

On the basis of both natural samples and experimental studies, clinopyroxene is a potential reservoir for potassium in the Earth's mantle. The amount of K partitioning into clinopyroxene depends on the phase assemblage present, the bulk composition, pressure, and temperature. To investigate some of these dependencies, subsolidus and melting phase relations in the system phlogopite-diopside have been studied to 17 GPa. In this system, phlogopite becomes unstable with increasing pressure, breaking down to potassium richterite, which in turn breaks down to another K-bearing hydrous phase (phase X), such that a K-rich phase coexists with clinopyroxene to 17 GPa. Clinopyroxenes contain ≤1.3 wt% $K_2O$ in assemblages of phlogopite + clinopyroxene ± olivine ± liquid at 3–5 GPa, phlogopite + clinopyroxene + garnet ± olivine ± liquid at 7–9 GPa, clinopyroxene + garnet + olivine ± potassium richterite ± liquid at 11 GPa, and clinopyroxene + olivine + garnet + phase X at 14 and 17 GPa.

In these assemblages, K is partitioned into hydrous phases or liquid, rather than into the clinopyroxene. By inference, phlogopite (or its higher-pressure breakdown products) is the primary host for K in the mantle (if $H_2O$ is present), and any coexisting clinopyroxene has very low concentrations of K. Conversely, the natural occurrence of clinopyroxene with >> 1 wt% $K_2O$ requires that phlogopite, potassium richterite, or phase X is not stable in the local source environment of such samples.

## INTRODUCTION

The nature and stability of hosts for volatiles such as $H_2O$ and $CO_2$ in the Earth's mantle are important because of the effects of volatiles on physical properties of the mantle and on melting processes. Modeling the geochemical cycles for volatile components such as $H_2O$ and $CO_2$ require consideration of the mantle part of the cycle, because subduction processes potentially return volatiles to the mantle and because the mantle is degassing at divergent plate boundaries and at intraplate settings. The potential stability of hydrous and carbonate minerals in the mantle has obvious implications for this modeling and hence to the question of the temporal evolution of the (surface) hydrosphere. Phlogopite has been a popular candidate for storage of $H_2O$ because it is stable to pressures > 10 GPa (Sudo and Tatsumi 1990) at temperatures thought to be appropriate for the upper mantle, based on current models of the geotherm. Examination of the behavior of K is required both because of its role in stabilizing hydrous phases such as phlogopite and because it contributes to the internal heat budget of the Earth by means of radioactive decay of $^{40}K$.

This study was designed with three objectives in mind. First, subsequent to the discovery of clinopyroxene containing >1.5 wt% $K_2O$ (Harlow and Veblen 1991), experiments are desirable to measure the K content of clinopyroxene coexisting with other K-bearing phases. Second, this is a simple system in which to examine potential dehydration-melting reactions relevant to both pyroxenite and peridotite assemblages in the mantle. Third, it is of interest to evaluate the pressure-dependent breakdown reactions of phlogopite and potassium richterite, which is formed by the breakdown of phlogopite.

### Potassic phases in the Earth's mantle

Phlogopite, because of its occurrence in mantle-derived xenoliths (cf. Dawson 1980), is a logical candidate as a potential host for K and $H_2O$ in the Earth's upper mantle. Recently, Rosenbaum (1993) drew attention to the presence of high (>1.5 ppm) concentrations of Pb in phlogopite from mantle xenoliths, and he pointed out that phlogopite could be a significant reservoir for Pb in the upper mantle, providing another rationale for further study of the stability of this phase in mantle mineral assemblages.

A significant constraint on the modal abundance of phlogopite in average mantle peridotite is the low abundance of $K_2O$ in such rocks. Most models of undepleted (and unenriched) mantle lherzolite contain ~0.03 wt% $K_2O$ (e.g., Ringwood 1979; Hart and Zindler 1986; McDonough and Sun 1995; Allègre et al. 1995). K contents of peridotite xenoliths are variable, and secondary phlogopite, which inflates the $K_2O$ content above primitive mantle values, is often present in these xenoliths. For

0003–004X/97/1112–1198$05.00

example, the xenolith PHN 1611 contains 0.14 wt% $K_2O$ (Nixon and Boyd 1973), and a suite of peridotite xenoliths from southern Africa were found to contain 0.01 to 0.44 wt% $K_2O$ (Boyd and Mertzman 1987). These authors explicitly addressed the problem of secondary minerals by recalculating whole-rock compositions based on modal abundances and compositions of primary minerals. These recalculated compositions are essentially $K_2O$-free (e.g., Table 3 of Boyd and Mertzman 1987). Patently metasomatic phlogopite-bearing peridotites may contain >2.0 wt% $K_2O$ (Erlank et al. 1987), and MARID (mica + amphibole + rutile + ilmenite + diopside) xenoliths may contain up to 8 wt% $K_2O$ (Waters 1987; Erlank et al. 1987; Sweeney et al. 1993).

The heterogeneity of subcontinental mantle, as evidenced by the compositional and mineralogical variability in the xenolith suites, justifies further study of phlogopite, as does the potential of subduction to provide a conduit for more K-rich material to be recycled into the mantle (e.g., Plank and Langmuir 1993; von Huene and Scholl 1991; Irifune et al. 1994).

Clinopyroxene has been proposed as a host for K in mantle-derived rocks, following the original suggestion of Erlank (1970), based on his measurements of 800 to 1350 ppm $K_2O$ in omphacitic clinopyroxene. Subsequent studies of omphacite from mantle xenoliths and from diamond inclusions with electron microprobe (e.g., Reid et al. 1976; Bishop et al. 1978; McCandless and Gurney 1989) and with analytical transmission electron microscopy (Harlow and Veblen 1991) confirm that some clinopyroxene samples contain up to 1.71 wt% $K_2O$ in solid solution. Clinopyroxene, especially in eclogitic assemblages, shows a rich complexity of composition, deviations from stoichiometry, and exsolution textures.

Exsolution lamellae of garnet or kyanite have been reported in omphacitic clinopyroxene from mantle-derived eclogites (e.g., Smyth et al. 1989). Quartz exsolution has been reported from clinopyroxene in Norwegian eclogites (Smith 1984; cf. review by Smith 1988). Exsolution of garnet implies that the precursor clinopyroxene contained significant Al in Tschermak's substitution:

$$\underset{\text{cpx}}{CaAl_2SiO_6} + \underset{\text{cpx}}{CaMgSi_2O_6} \rightarrow \underset{\text{garnet}}{(Ca_2Mg)Al_2Si_3O_{12}}.$$

Exsolution of either kyanite or quartz requires nonstoichiometry in the clinopyroxene, with solid solution toward the Ca-Eskola component ($Ca_{0.5}\square_{0.5}AlSi_2O_6$, where $\square$ represents a vacancy on the M2 site) being a reasonable possibility (Smyth et al. 1989). It has been demonstrated experimentally that high-silica environments are required to generate clinopyroxene with significant Ca-Eskola component (Wood and Henderson 1978; Gasparik 1986).

Of particular interest in the present context is the report of blebs of a K-rich phase of feldspar stoichiometry found in clinopyroxenes from diamondiferous eclogites by Reid et al. (1976). If these blebs exsolved from a precursor single phase, both a Ca-Eskola component and a ''K-jadeite'' ($KAlSi_2O_6$) component are required:

$$\underset{\text{cpx}}{3KAlSi_2O_6} + \underset{\text{cpx}}{2Ca_{0.5}\square_{0.5}AlSi_2O_6} = \underset{\text{feldspar}}{3KAlSi_3O_8} + \underset{\text{cpx}}{CaAl_2SiO_6}.$$

Cation-deficient pyroxenes are stable at conditions found in the mantle, as evidenced by their occurrence in kimberlites (Smyth 1980) and by recent experiments on the phase relationships of an anhydrous basaltic bulk composition (Yasuda et al. 1994). Clinopyroxenes from these experiments contain up to ~14% of a Ca-Eskola component. Experimental work reported by Harlow (1996a) documents the complex relationships between the mineral assemblage present, especially the aluminous phase, and the presence of vacancies, Ca-Tschermak's substitution, and high K content in clinopyroxenes.

Although cation deficiency per se is not required for K substitution, such vacancies may provide localized strain relief to facilitate substitution of K into the pyroxene structure. Other mechanisms may allow K substitution into clinopyroxene. Harlow and Veblen (1991) suggested that K would more readily substitute into clinopyroxenes with larger unit-cell volumes. They further proposed that substitution of larger $Cr^{3+}$ or $Fe^{3+}$ for $Al^{3+}$ in the M1 site helps expand the M2 site to accommodate K. On the basis of a crystal structure refinement of a natural K-rich clinopyroxene, Harlow (1996b) suggested that substitution of Mg into the M2 site would facilitate K substitution. Because Mg is smaller than Ca, small M2 polyhedra occupied by Mg could compensate for larger M2 polyhedra containing K. Harlow (1997) found evidence to support several mechanisms to accommodate K in clinopyroxene such as a large average M2 site, coupled substitution of K and smaller cations in M2, and a larger cation ($Cr^{3+}$) in M1. He further proposed that the polyhedral compressibility of Na and K are large in comparison with Ca, and hence Na and K decrease in size more with increasing pressure. This explanation explicitly addresses the observed increase in K content of clinopyroxene with increasing pressure.

## Previous experimental studies on phlogopite-pyroxene phase relationships

Kushiro et al. (1967) determined that a natural phlogopite was stable to 7.2 GPa at 1000 °C. Yoder and Kushiro (1969) found that the assemblage forsterite + phlogopite was stable to at least 3.75 GPa at 1200 °C. Kushiro (1970) studied the stability of phlogopite + enstatite and phlogopite + diopside and determined that phlogopite was stable at 3.3 GPa, 1100 °C and 3.2 GPa, 1000 °C, respectively. In both cases, he found forsterite + quenched vapor (or liquid) in the experimental products, and attributed the presence of the forsterite to preferential dissolution of K and Al in the vapor. The stoi-

chiometries of phlogopite and forsterite require that Si dissolved preferentially relative to Mg as well.

Modreski and Boettcher (1972) studied the stability of phlogopite + enstatite assemblages to 3.0 GPa. In a subsequent study on the melting relationships of phlogopite coexisting with one or more of the phases forsterite, enstatite, diopside, spinel, pyrope, and corundum, Modreski and Boettcher (1973) determined the phase relations of phlogopite + enstatite (± excess $H_2O$) and phlogopite + diopside (± excess $H_2O$) to 3.5 GPa. In both cases, phlogopite was stable to the highest pressure studied, and K contents of the clinopyroxene in the latter experiments were very low (<0.5 wt%).

In experiments reported in abstract form and briefly summarized in Luth et al. (1993), Trønnes (1990) studied the phase relations of pure phlogopite and phlogopite peridotite, finding that in both cases phlogopite broke down at pressures of ~7 GPa to potassium richterite bearing assemblages, which in turn broke down at higher pressures (~13 GPa) to assemblages containing a high-K, low-Al hydrous phase, which was interpreted as an amphibole, based on its chemical composition, stoichiometry, and powder X-ray diffraction pattern.

Sudo and Tatsumi (1990) studied the phase relations of phlogopite + diopside ± enstatite at pressures from 5 to 13 GPa, and at temperatures of 1000 to 1300 °C. With increasing pressure, their studies of phlogopite + diopside found the phase assemblages to be phlogopite + diopside (5.0 and 5.9 GPa), phlogopite + diopside + garnet (6.5 and 7.4 GPa), phlogopite + diopside + garnet + forsterite + amphibole ± vapor (9.3 and 11.1 GPa), and diopside + garnet + forsterite + amphibole + vapor (11.1 and 13 GPa). They suggested that the coexistence of amphibole and clinopyroxene reflected the divariant nature of the phlogopite + diopside breakdown reaction. They published analyses for garnet ($Mg_{2.552}Ca_{0.592}Al_{1.682}Si_{3.167}O_{12}$) and amphibole [$K_{1.917}Ca_{1.082}Mg_{5.010}Al_{0.132}Si_{7.876}O_{22}(OH)_2$] from one experiment, but not for the clinopyroxenes from their experimental products.

### Rationale for studying dehydration melting reactions

A popular mechanism to generate melting in the lower crust is to flux it with $H_2O$ provided by breakdown of hydrous silicates, such as micas and amphiboles (cf. discussion in Thompson and Connolly 1995). Such behavior has been termed ''dehydration melting'' to emphasize the role that the hydrous phase(s) play in allowing melting at lower temperatures than possible for the analogous anhydrous assemblage. Melting occurs by this mechanism at higher temperatures than it would in the presence of an $H_2O$-rich vapor.

Similarly, dehydration-melting reactions could flux melting in the mantle at temperatures lower than those for anhydrous melting. Dehydration melting is relevant to the mantle because of the results of the studies of the vapor-present melting in $MgO$-$SiO_2$-$H_2O$ at 3 to 12 GPa by Luth (1993) and at 5.5 to 15.5 GPa by Inoue (1994), and at 16 to 23 GPa by Gasparik (1993). These studies demonstrate that the wet solidus of forsterite would intersect a mantle geotherm at 4 to 6 GPa and would remain at temperatures lower than the geotherm to >23 GPa. The lack of seismic evidence for widespread melting at depths below ~150 km implies that a free $H_2O$-rich fluid is not present. Dehydration melting, then, must be considered as a possible mechanism that allows localized melting at temperatures below the dry solidus of anhydrous peridotite. To evaluate the relevance to the mantle of dehydration melting in phlogopite-bearing assemblages, the solidus phase relationships are determined for phlogopite + clinopyroxene assemblages.

**TABLE 1.** Compositions of starting materials

| | Phlogopite ($n$ = 30) | Diopside glass ($n$ = 12) |
|---|---|---|
| | **Weight percentages** | |
| $SiO_2$ | 43.1(4) | 56.5(4) |
| $Al_2O_3$ | 12.2(3) | 0.0 |
| MgO | 28.3(3) | 18.3(2) |
| CaO | 0.0 | 25.7(1) |
| $K_2O$ | 11.2(3) | 0.0 |
| Total | 94.9(6) | 100.6(5) |
| **Cations per 22 O** | | **cations per 6 O** |
| Si | 6.037 | 2.020 |
| Al | 2.018 | 0.000 |
| Mg | 5.897 | 0.976 |
| Ca | 0.000 | 0.983 |
| K | 2.004 | 0.000 |

*Notes:* $n$ = number of analyses. Standard deviations in the last digit are given in parentheses.

## EXPERIMENTAL PROCEDURE

The starting material used for the experiments was a mixture of synthetic diopside glass and crystalline phlogopite. The diopside glass was synthesized from a mixture of high-purity (≥99.95% purity) $CaCO_3$, MgO, and $SiO_2$. The mixture was decarbonated at 800 °C for 3 h, then melted at 1450 °C for 3 h, quenched, ground, and remelted at 1450 °C for an additional 4 h, followed by quenching in liquid $N_2$. The analyses for the synthetic glass (Table 1) show a slight excess of $SiO_2$ over ideal diopside composition. The phlogopite starting material was synthesized from an oxide-carbonate mixture. The mixture was encapsulated in a welded 5 mm diameter platinum capsule together with 7 wt% $H_2O$ and run in a 19 mm diameter talc-pyrex furnace assembly (Kushiro 1976) at 1.5 GPa, 1000 °C for 48 h in an end-loaded piston-cylinder apparatus. The synthesized phlogopite was characterized by electron microprobe analysis (Table 1) and by powder X-ray diffraction, which showed only mica. A 50:50 (w/w) mixture of the glass and mica was homogenized by mixing under ethanol in an agate mortar and pestle for ~30 min. After drying under a heat lamp, the mixture was stored in a desiccator over KOH until used.

The samples for all experiments were placed in platinum capsules that were sealed by welding after drying the enclosed mixture at 120 °C for 12–16 h. The capsules

**TABLE 2.** Run conditions and phase assemblages

| *P* (GPa) | *T* (°C) | Duration (h) | Experiment no. | Phase assemblage |
|---|---|---|---|---|
| 3 | 1250 | 1 | 1207 | Ph + Cpx + Ol |
| 3 | 1250 | 6 | 1181 | Ph + Cpx + Ol |
| 3 | 1325 | 6 | 1182 | Cpx + Ol + L |
| 5 | 1200 | 10 | 1209 | Ph + Cpx |
| 5 | 1300 | 6 | 1180 | Ph + Cpx + Ol |
| 5 | 1350 | 12 | 1183 | Ph + Cpx + Ol |
| 5 | 1400 | 6 | 1179 | Cpx + Ol + L |
| 5 | 1500 | 4 | 1178 | Cpx + Ol + L |
| 7.5 | 1300 | 6 | 994 | Ph + Cpx + Ol + Gar |
| 7.5 | 1400 | 10 | 1214 | Ph + Cpx + Ol + Gar |
| 7.5 | 1450 | 8 | 1208 | Cpx + Ol + Gar + L |
| 7.5 | 1550 | 8 | 1213 | Cpx + Ol + Gar + L |
| 9 | 1450 | 8 | 1215 | Cpx + Ol + Gar + L |
| 9 | 1500 | 8 | 1212 | Cpx + Ol + Gar + L |
| 9 | 1550 | 8 | 1211 | Cpx + Ol + Gar + L |
| 11 | 1300 | 8 | 1107 | ol + gar + cpx + amph |
| 11 | 1600 | 4 | 1106 | ol + cpx + gar + Phase X + L |
| 11 | 1600 | 8 | 1163 | ol + gar + cpx + L |
| 14 | 1300 | 8 | 1105 | ol + gar + cpx + Phase X |
| 14 | 1600 | 8 | 1104 | ol + gar + cpx + Phase X |
| 17 | 1600 | 8 | 1221 | cpx + Phase X + gar |

*Note:* Abbreviations: ol = olivine, ph = phlogopite, cpx = clinopyroxene, gar = garnet, amph = amphibole, Phase X = unknown K-bearing hydrous phase (see text for discussion).

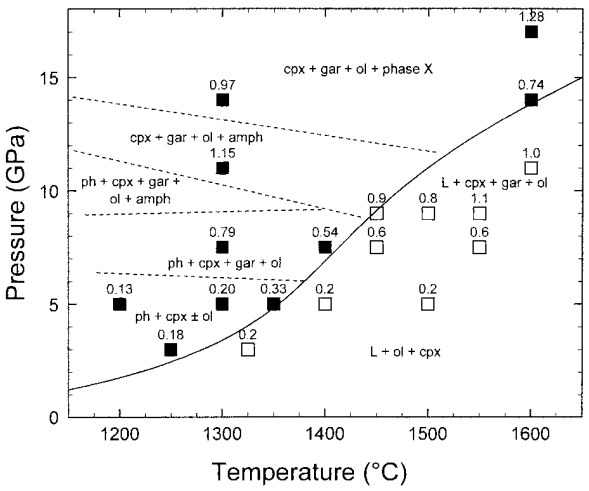


**FIGURE 1.** Pressure-temperature projection of experimental results. Solid curve is the inferred solidus. Numbers on top of each datum are the concentration of $K_2O$, in weight percent, in the clinopyroxene at each condition. Solid squares are subsolidus experiments; open squares are supersolidus experiments. Fields for stable phase assemblages shown are based on the results of this study (Table 2), on the results of Sudo and Tatsumi (1990) at lower temperatures, and on the results of Modreski and Boettcher (1973) at lower pressures (see Fig. 2).

were compressed gently into a cylindrical shape in a steel die to minimize void space in the sample assembly.

At pressures below 10 GPa, capsules of 1.5 mm diameter were experimented on in sample assemblies consisting of a stepped graphite furnace surrounded by a $ZrO_2$ sleeve, inner MgO and $Al_2O_3$ spacers, and an axial $W_{97}Re_3$-$W_{75}Re_{25}$ or $W_{95}Re_5$-$W_{74}Re_{26}$ thermocouple, all contained within a semi-sintered $Cr_2O_3$-MgO octahedron of 18 mm edge length. At 10–14 GPa, the capsules were 1.5 mm diameter, and sample assemblies were similar, but with a stepped $LaCrO_3$ furnace and an octahedron of 14 mm edge length. The 17 GPa experiments were run in 1.0 mm diameter platinum capsules in a 10 mm octahedron with a straight $LaCrO_3$ furnace design and an axial $W_{97}Re_3$-$W_{75}Re_{25}$ thermocouple. Temperature gradients from center to end of the sample capsule were ~20, ~40, and ~100 °C in the 18, 14, and 10 mm sample assemblies, respectively. Further details of the sample assemblies, thermal gradients, and pressure calibration techniques are in Walter et al. (1995). All experiments were run in the USSA-2000 multiple-anvil apparatus at the University of Alberta.

Samples were brought to the experiment pressure, then heated at ~70 °C/min to experiment temperature, and maintained at the temperature with a precision of ±5 °C. No correction was applied to the emf of the thermocouple. The experiments were quenched by turning off the power to the furnace, resulting in a temperature drop to <300 °C in 2–5 s. For the lower-temperature experiments, the capsule was sectioned with a diamond wafering blade. One side was cast in an 2.54 cm diameter epoxy plug, ground, and polished for electron microprobe analysis. The other side of the capsule was archived for future analytical studies. For the near-solidus experiments, where problems with plucking and the preservation of textures were pervasive, the unopened capsule was cast in the epoxy plug. The plug was then ground down until the capsule wall was breached, then vacuum-assisted epoxy impregnation was used to help preserve the textures. The samples were then polished for microprobe analyses.

Microprobe analyses were done on the JEOL 8900 microprobe at the University of Alberta, using wavelength-dispersive analysis. Analytical conditions were 15 kV accelerating voltage and a focused (spot) beam with cup beam current of 15 nA. During analysis of glass, the beam diameter was expanded to 5–10 μm, depending on the size of the glass region, to mitigate problems analyzing these hydrous, K-rich glasses. Beam current on the sample was 10–12 nA. Natural augite and synthetic diopside were used as standards for Ca, Mg, and Si in the pyroxene; natural sanidine was used for K and Al standards for the pyroxenes. A synthetic fluorophlogopite was used for K, Mg, Al, and Si in the micas. Natural ($Fo_{93}$) olivine was used as a standard for the experimental olivines. For the analyses of garnet, natural grossular- and pyrope-rich garnets were used as standards. The microprobe data were reduced using the CITZAF program provided by JEOL.

## RESULTS

### General

The phase assemblages and conditions for all experiments are given in Table 2, and are illustrated in Figure 1. The number on top of each datum in Figure 1 is the concentration of $K_2O$ (in wt%) in the clinopyroxenes

**TABLE 3.** Compositions of clinopyroxenes

| | | | | | | | |
|---|---|---|---|---|---|---|---|
| *P* (GPa) | 3 | 3 | 3 | 5 | 5 | 5 | 5 |
| *T* (°C) | 1250 | 1250 | 1325 | 1200 | 1300 | 1350 | 1400 |
| Expt. no. | 1207 | 1181 | 1182 | 1209 | 1180 | 1183 | 1179 |
| *n* | 16 | 20 | 9 | 14 | 16 | 19 | 10 |
| $SiO_2$ | 55.4(2) | 55.1(2) | 54.2(2) | 55.5(2) | 54.8(2) | 54.2(3) | 54.2(3) |
| $Al_2O_3$ | 0.6(1) | 0.6(1) | 2.0(5) | 0.2(1) | 0.7(2) | 1.4(3) | 2.7(1) |
| MgO | 19.7(3) | 20.4(3) | 19.5(1) | 19.0(2) | 19.8(5) | 20.4(3) | 20.5(2) |
| CaO | 23.9(3) | 23.7(3) | 23.5(4) | 24.9(3) | 23.8(5) | 23.0(4) | 21.7(1) |
| $K_2O$ | 0.3(1) | 0.18(8) | 0.17(2) | 0.13(3) | 0.20(3) | 0.3(2) | 0.24(5) |
| Total | 99.8(4) | 100.1(3) | 99.4(2) | 99.8(3) | 99.3(4) | 99.3(4) | 99.4(4) |
| | | | **Cations per 6 O atoms** | | | | |
| Si | 1.990(4) | 1.976(5) | 1.955(8) | 2.000(3) | 1.981(6) | 1.959(6) | 1.946(5) |
| Al | 0.026(6) | 0.027(3) | 0.09(2) | 0.009(3) | 0.028(7) | 0.06(1) | 0.116(6) |
| Mg | 1.06(2) | 1.09(2) | 1.049(6) | 1.023(8) | 1.07(2) | 1.10(1) | 1.097(8) |
| Ca | 0.92(1) | 0.91(1) | 0.91(2) | 0.96(1) | 0.92(2) | 0.89(2) | 0.833(6) |
| K | 0.013(6) | 0.008(4) | 0.008(1) | 0.006(1) | 0.009(2) | 0.015(7) | 0.011(2) |
| Total | 4.004(3) | 4.014(5) | 4.006(3) | 3.999(4) | 4.010(5) | 4.020(5) | 4.002(3) |
| | | | **End-member components** | | | | |
| KCpx | 0.013 | 0.008 | 0.008 | 0.006 | 0.009 | 0.015 | 0.011 |
| CaTs | 0.006 | 0.009 | 0.039 | 0.001 | 0.010 | 0.021 | 0.052 |
| Di | 0.910 | 0.890 | 0.864 | 0.961 | 0.905 | 0.851 | 0.778 |
| En | 0.071 | 0.093 | 0.090 | 0.031 | 0.076 | 0.113 | 0.158 |

*Note:* $n$ = number of analyses. Standard deviations in the last digit(s) are given in parentheses. KCpx = $KAlSi_2O_6$; CaTs = $CaAl_2SiO_6$; Di = $CaMgSi_2O_6$; En = $Mg_2Si_2O_6$.

present in the experiment. The subsolidus experiments tended to have a fine-grained ($\leq$ 10 $\mu$m) texture, with no noticeable systematic variation in grain size across the sample. No conspicuous phase segregation from thermal compaction (Harlow 1997) was observed. The supersolidus experiments often showed segregation of the liquid to the hotter portion of the capsule, accompanied by larger grains near the solid-liquid interface.

The phases present did not have any compositional zoning that was observable in back-scattered electron imaging; the small grain size of the subsolidus experimental products prohibited systematic core and rim analyses. In coarser-grained (supersolidus) experiments, compositional zoning within grains was not systematic, if present, and was not outside the range of grain-to-grain variability. There was some grain-to-grain variability, as is evidenced by the uncertainties (Tables 3–5), which are larger than expected from counting statistics alone.

### Clinopyroxene

In all experiments, the clinopyroxene grains produced are stoichiometric (Table 3), indicating that vacancies are not a requirement for moderate amounts of incorporation of K into the pyroxene structure. In the supersolidus region, there is a clear increase of $K_2O$ in the clinopyroxene with increasing pressure, up to 1.0 wt% at 11 GPa (Table 3). In the subsolidus region, there is a general increase in $K_2O$ content with pressure, but the decrease between 11 and 14 GPa reflects the importance of the nature of the coexisting K-rich phase on the K content of the clinopyroxene. The Al content of the clinopyroxene increases with increasing temperature at each pressure.

### K-bearing hydrous phases

The compositions of the micas have Al > 2 cations per 22 O atoms, reflecting a character intermediate between trioctahedral and dioctahedral. Some systematic trends with pressure and temperature are apparent (Table 4). At 5 GPa, Mg in the mica decreases with increasing temperature. The micas become less K-rich and more Si- and Mg-rich between 5 and 7.5 GPa at 1300 °C. The low total for the mica at 7.5 GPa may indicate excess protons in the structure (e.g., Robert et al. 1995), but further work is required to confirm this. The composition of the potassium richterite (experiment at 11 GPa) is consistent with previous studies (Sudo and Tatsumi 1990). The composition of hydrous phase X found in experiments at 14 and 17 GPa is similar to those previously reported by Trønnes (1990) and Inoue et al. (1995). The nature and significance of this phase is discussed below.

### Garnet

The garnet grains (Table 5) are high-Mg (Mg/(Mg + Ca) > 0.80), similar to that reported by Sudo and Tatsumi (1990). The consistent presence of more than 3.00 cations of Si per 12 O atoms requires the presence of a majorite component ($^{[8]}M_3{}^{[6]}M^{[6]}Si_3{}^{[4]}O_{12}$, where M = Ca or Mg). The amount of majorite component increases with increasing pressure, as expected from previous work in garnet-pyroxene systems (Ringwood 1967; Akaogi and Akimoto 1977; Liu 1977; Kanzaki 1987).

### Olivine

The olivine is stoichiometric within analytical uncertainty and has very little K, Ca, or Al substituting in it ($K_2O \leq 0.1$, $CaO \leq 0.4$, $Al_2O_3 \leq 0.2$ wt%, with uncertainties on the same order as the concentrations). No systematic behavior of Ca or Al was observed with changing pressure or temperature, which reflect the low concentrations of these cations and attendant high relative uncertainties.

**TABLE 3**—*Extended*

| *P* (GPa) | 5 | 7.5 | 7.5 | 7.5 | 7.5 | 9 | 9 |
|---|---|---|---|---|---|---|---|
| *T* (°C) | 1500 | 1300 | 1400 | 1450 | 1550 | 1450 | 1500 |
| Expt. no. | 1178 | 994 | 1214 | 1208 | 1213 | 1215 | 1212 |
| *n* | 11 | 8 | 10 | 12 | 11 | 15 | 10 |
| $SiO_2$ | 54.4(3) | 55.4(2) | 54.9(2) | 55.1(1) | 55.3(2) | 55.6(2) | 55.2(2) |
| $Al_2O_3$ | 2.2(3) | 1.2(1) | 1.1(5) | 1.5(2) | 1.7(1) | 1.3(2) | 1.4(2) |
| MgO | 20.5(4) | 19.4(3) | 19.7(4) | 20.2(3) | 21.1(2) | 20.5(2) | 20.1(4) |
| CaO | 21.9(6) | 22.8(1) | 23.9(9) | 22.5(6) | 21.0(2) | 22.2(7) | 22.0(7) |
| $K_2O$ | 0.19(3) | 0.79(6) | 0.5(1) | 0.6(1) | 0.6(1) | 0.9(1) | 0.8(2) |
| Total | 99.1(4) | 99.6(4) | 100.2(3) | 99.9(2) | 99.7(4) | 100.5(5) | 99.4(4) |
| **Cations per 6 O atoms** | | | | | | | |
| Si | 1.958(7) | 1.993(4) | 1.971(9) | 1.976(4) | 1.976(4) | 1.982(5) | 1.984(4) |
| Al | 0.09(1) | 0.051(4) | 0.05(2) | 0.062(9) | 0.073(3) | 0.053(9) | 0.058(9) |
| Mg | 1.10(2) | 1.04(1) | 1.05(2) | 1.08(2) | 1.123(7) | 1.09(1) | 1.08(2) |
| Ca | 0.84(2) | 0.879(7) | 0.92(4) | 0.86(3) | 0.802(8) | 0.85(3) | 0.85(3) |
| K | 0.009(1) | 0.036(3) | 0.025(6) | 0.027(4) | 0.029(3) | 0.042(6) | 0.037(7) |
| Total | 4.001(4) | 4.000(4) | 4.018(6) | 4.007(4) | 4.003(3) | 4.013(5) | 4.005(4) |
| **End-member components** | | | | | | | |
| KCpx | 0.009 | 0.036 | 0.024 | 0.027 | 0.029 | 0.041 | 0.037 |
| CaTs | 0.041 | 0.007 | 0.011 | 0.017 | 0.022 | 0.005 | 0.011 |
| Di | 0.802 | 0.872 | 0.893 | 0.841 | 0.778 | 0.831 | 0.834 |
| En | 0.148 | 0.084 | 0.071 | 0.115 | 0.171 | 0.122 | 0.118 |

## Liquid

The liquids generated by dehydration melting of phlogopite contain some contribution from the coexisting clinopyroxene as well, as evidenced by their CaO content (Table 6). No satisfactory analyses of liquid could be obtained at low melt fractions because of the small size of the interstitial melt pockets and the problems of plucking in those samples. Even at higher melt fractions, considerable scatter was found in the liquid analyses. This scatter is attributed to the presence of quench phases, and the commonly interstitial nature of the melt in many experiments. Liquid was not observed to coexist with phlogopite in any experiment.

The melt fraction was estimated, albeit with considerable uncertainty, in two ways. The first assumed that the entire deficiency of the total of the microprobe analysis can be attributed to $H_2O$ in the quench liquid. These values (melt fraction from Δtotal in Table 6) suffer from the problem that all the analytical uncertainties that contributes to totals differing from 100% propagate through to the calculated liquid proportion. For example, these values require an implausible decrease in melt fraction with a 100 °C increase in temperature at 7.5 GPa.

An alternative technique used mass balance constraints. The compositions of the starting material and the phases present in the quenched experiment were used in a least-squares regression mixing model to infer the proportions of the phases involved. These values are given in the melt

**TABLE 3**—*Continued*

| *P* (GPa) | 9 | 11 | 11 | 11 | 14 | 14 | 17 |
|---|---|---|---|---|---|---|---|
| *T* (°C) | 1550 | 1300 | 1600 | 1600 | 1300 | 1600 | 1600 |
| Expt. no. | 1211 | 1107 | 1106 | 1163 | 1105 | 1104 | 1221 |
| *n* | 7 | 15 | 13 | 10 | 12 | 13 | 20 |
| $SiO_2$ | 55.1(3) | 55.0(7) | 55.8(4) | 55.2(2) | 55.4(2) | 55.5(3) | 55.0(3) |
| $Al_2O_3$ | 1.5(1) | 1.3(2) | 1.4(1) | 1.4(1) | 0.9(2) | 1.1(3) | 0.9(3) |
| MgO | 20.1(7) | 18.3(4) | 20.6(3) | 20.5(3) | 19.8(3) | 20.7(3) | 19.5(2) |
| CaO | 21.6(5) | 22.8(9) | 21.0(3) | 21.0(3) | 22.4(7) | 21.1(6) | 23.2(4) |
| $K_2O$ | 1.1(1) | 1.2(3) | 1.0(1) | 0.8(1) | 1.0(2) | 0.7(1) | 1.3(3) |
| Total | 99.4(3) | 98.5(1.2) | 99.7(5) | 98.9(2) | 99.4(2) | 99.1(4) | 100.0(3) |
| **Cations per 6 O atoms** | | | | | | | |
| Si | 1.983(4) | 2.004(7) | 1.995(5) | 1.991(3) | 1.998(3) | 1.997(7) | 1.983(5) |
| Al | 0.064(4) | 0.054(9) | 0.057(3) | 0.060(2) | 0.037(6) | 0.05(1) | 0.04(1) |
| Mg | 1.08(3) | 0.99(1) | 1.098(2) | 1.101(1) | 1.06(2) | 1.11(2) | 1.05(1) |
| Ca | 0.84(2) | 0.89(3) | 0.81(1) | 0.81(1) | 0.86(3) | 0.81(2) | 0.90(2) |
| K | 0.051(6) | 0.05(1) | 0.045(2) | 0.036(3) | 0.045(7) | 0.034(4) | 0.06(1) |
| Total | 4.010(3) | 3.995(7) | 3.999(4) | 3.997(3) | 4.006(4) | 3.997(3) | 4.027(6) |
| **End-member components** | | | | | | | |
| KCpx | 0.051 | 0.054 | 0.045 | 0.036 | 0.044 | 0.034 | 0.057 |
| CaTs | 0.006 | 0.000 | 0.006 | 0.012 | −0.004 | 0.006 | −0.009 |
| Di | 0.820 | 0.894 | 0.799 | 0.800 | 0.862 | 0.808 | 0.882 |
| En | 0.123 | 0.052 | 0.150 | 0.152 | 0.097 | 0.152 | 0.070 |

**TABLE 4.** Compositions of K-bearing hydrous phases

| *P* (GPa) | 3 | 3 | 5 | 5 | 5 | 7.5 | 7.5 |
|---|---|---|---|---|---|---|---|
| *T* (°C) | 1250 | 1250 | 1200 | 1300 | 1350 | 1300 | 1400 |
| Expt. no. | 1207 | 1181 | 1209 | 1180 | 1183 | 994 | 1214 |
| Phase | mica | mica | mica | mica | mica | mica | mica |
| *n* | 26 | 10 | 19 | 15 | 10 | 12 | 10 |
| $SiO_2$ | 42.2(6) | 42.3(3) | 42.2(9) | 42.5(3) | 41.6(8) | 43.6(3) | 43.7(4) |
| $Al_2O_3$ | 12.9(7) | 12.6(2) | 13.3(15) | 12.7(3) | 13.8(4) | 12.3(2) | 12.7(3) |
| MgO | 28.3(3) | 28.5(8) | 28.3(5) | 28.1(2) | 27.3(5) | 29.0(2) | 27.3(4) |
| CaO | 0.1(1) | 0.1(1) | 0.1(1) | 0.1(1) | 0.1(1) | 0.0(0) | 0.0(0) |
| $K_2O$ | 11.2(3) | 11.6(5) | 11.5(1) | 11.7(1) | 12.4(4) | 9.4(2) | 11.5(1) |
| Total | 94.6(7) | 95.1(4) | 95.4(4) | 95.0(5) | 95.2(13) | 94.3(4) | 95.3(7) |
| | | | | **Cations** | | | |
| Si | 5.93(7) | 5.94(5) | 5.9(1) | 5.97(3) | 5.85(4) | 6.06(2) | 6.08(4) |
| Al | 2.13(12) | 2.08(4) | 2.2(2) | 2.10(5) | 2.29(7) | 2.02(3) | 2.09(5) |
| Mg | 5.92(7) | 5.95(15) | 5.90(11) | 5.87(3) | 5.7(1) | 6.01(2) | 5.67(5) |
| Ca | 0.010(3) | 0.02(2) | 0.011(4) | 0.010(4) | 0.01(1) | 0.01(1) | 0.00(0) |
| K | 2.01(5) | 2.08(9) | 2.04(2) | 2.10(2) | 2.23(5) | 1.66(3) | 2.04(2) |
| Total cations | 16.01(4) | 16.07(3) | 16.03(3) | 16.04(1) | 16.12(3) | 15.76(3) | 15.89(4) |
| No. of O: | 22 | 22 | 22 | 22 | 22 | 22 | 22 |

*Note: n* = number of analyses. Standard deviations in the last digit(s) are given in parentheses.

fraction ''from modal min'' row in Table 6. These results have the merit of at least the right sense of increasing melt fraction with increasing temperature. It is worth noting that both techniques yield large degrees of partial melting in these experiments, consistent with qualitative visual inspection of the experimental products.

Despite the problems with estimating the proportion of melt, several general observations can be made regarding the evolution of the composition of the liquid with temperature at various pressures. Both $K_2O$ and $Al_2O_3$ decrease with increasing temperature and CaO increases with increasing temperature (compare 5 GPa experiments at 1400 vs. 1500 °C, and 7.5 GPa experiments at 1450° vs. 1550 °C). These results are consistent with phlogopite dominating the melting initially, with the clinopyroxene acting as a more refractory phase that dilutes the initial K- and Al-rich liquid with increasing temperature.

## DISCUSSION

### K contents of clinopyroxene

In these experiments, the chemical compositions of the clinopyroxene are consistent with K substituting into the pyroxene structure as a coupled substitution with Al, as a jadeite-like $KAlSi_2O_6$ component. The amount of K that dissolves in the pyroxene structure in these experiments is controlled by the presence and K content of coexisting K-rich phases, either mica, potassium richterite, phase X, or liquid. Quantitative modeling of buffering reactions requires thermochemical data for the fictitious $KAlSi_2O_6$ end-member in clinopyroxene. In the absence of such data, further discussion is premature.

Comparison of these results with those of Harlow (1997) illustrates the dependence of the K content of the clinopyroxene on the composition of the pyroxene and on the nature of the coexisting phase assemblage. The cli-

**TABLE 5.** Compositions of garnets

| *P* (GPa) | 7.5 | 7.5 | 7.5 | 7.5 | 9 | 9 | 9 |
|---|---|---|---|---|---|---|---|
| *T* (°C) | 1300 | 1400 | 1450 | 1550 | 1450 | 1500 | 1550 |
| Expt. no. | 994 | 1214 | 1208 | 1213 | 1215 | 1212 | 1211 |
| *n* | 7 | 7 | 13 | 18 | 10 | 11 | 10 |
| $SiO_2$ | 44.3(5) | 43.7(2) | 44.5(4) | 44.6(2) | 44.5(2) | 44.6(3) | 44.5(4) |
| $Al_2O_3$ | 23.4(5) | 22.7(3) | 23.1(8) | 23.5(4) | 22.7(3) | 23.1(3) | 22.9(6) |
| MgO | 23.3(3) | 22.9(5) | 23.3(5) | 23.7(4) | 24.0(4) | 23.6(5) | 25.2(4) |
| CaO | 8.1(5) | 8.3(5) | 8.4(8) | 7.9(5) | 7.5(4) | 8.0(6) | 6.1(8) |
| $K_2O$ | n.a. | 0.2(1) | 0.1(1) | 0.10(3) | 0.10(4) | 0.10(3) | 0.10(3) |
| Total | 99.1(5) | 97.7(4) | 99.3(2) | 99.7(3) | 98.8(3) | 99.3(3) | 98.8(5) |
| | | | | **Cations per 12 O atoms** | | | |
| Si | 3.06(3) | 3.07(2) | 3.07(3) | 3.07(2) | 3.087(9) | 3.08(2) | 3.08(3) |
| Al | 1.91(4) | 1.88(2) | 1.88(6) | 1.90(3) | 1.86(2) | 1.88(3) | 1.87(5) |
| Mg | 2.40(3) | 2.40(5) | 2.40(4) | 2.43(3) | 2.48(4) | 2.43(4) | 2.59(4) |
| Ca | 0.60(3) | 0.62(4) | 0.62(6) | 0.58(4) | 0.56(3) | 0.59(5) | 0.45(6) |
| K | n.a. | 0.014(4) | 0.010(9) | 0.004(3) | 0.009(3) | 0.006(3) | 0.007(3) |
| Total cations | 7.981(1) | 7.994(7) | 7.987(7) | 7.981(8) | 7.99(1) | 7.985(8) | 7.866(1) |

*Note: n* = number of analyses. Standard deviations in the last digit(s) are given in parentheses.

**TABLE 4**—*Extended*

| *P* (GPa) | 11 | 11 | 14 | 14 | 17 |
|---|---|---|---|---|---|
| *T* (°C) | 1300 | 1600 | 1300 | 1600 | 1600 |
| Expt. no. | 1107 | 1106 | 1105 | 1104 | 1221 |
| Phase | Amph | X | X | X | X |
| *n* | 6 | 1 | 6 | 6 | 6 |
| $SiO_2$ | 54.1(4) | 45.2 | 48.4(8) | 48.3(7) | 50.6(7) |
| $Al_2O_3$ | 2.4(2) | 9.2 | 2.1(2) | 2.0(5) | 1.7(1) |
| MgO | 23.1(2) | 26.4 | 30.3(6) | 30.4(10) | 28.3(10) |
| CaO | 7.9(6) | 0.5 | 0.4(1) | 0.4(2) | 0.5(2) |
| $K_2O$ | 7.8(4) | 10.2 | 13.6(5) | 12.9(5) | 15.4(8) |
| Total | 95.3(5) | 91.5 | 94.7(11) | 94.0(11) | 96.5(11) |
| | | | **Cations** | | |
| Si | 7.75(4) | 6.490 | 6.88(3) | 6.90(5) | 7.10(5) |
| Al | 0.41(3) | 1.550 | 0.35(4) | 0.33(9) | 0.29(2) |
| Mg | 4.94(6) | 5.670 | 6.43(7) | 6.5(1) | 5.9(1) |
| Ca | 1.22(9) | 0.080 | 0.06(2) | 0.06(3) | 0.07(2) |
| K | 1.43(8) | 1.880 | 2.5(1) | 2.4(1) | 2.8(2) |
| Total cations | 15.75(5) | 15.670 | 16.18(8) | 16.11(4) | 16.13(9) |
| No of O: | 23 | 22 | 22 | 22 | 22 |

nopyroxenes in his experiments contain Na in addition to K, and have generally higher K contents than those in the present study. Similar to the present study, however, his pyroxenes were not cation-deficient and substitution of K was charge-balanced by a trivalent M1 cation.

In light of the proposal of Harlow (1996b, 1997) that substitution of Mg on the M2 site could help compensate for the strain induced by substitution of K, a correlation between Mg on the M2 site and K was sought, but not found. No systematic correlation between K content and average M2 site size was observed (cf. Harlow 1996b). It is possible that such correlations are present but masked by the low concentrations of K in the clinopyroxenes in this study or the complicating effects of changing coexisting phase assemblages, which in turn induces changes in the Mg and Al content of the clinopyroxenes.

No generalization may be made about the temperature dependence of the $K_2O$ content of the pyroxene, possibly reflecting control by the different coexisting assemblages. For example, at 5 GPa where the subsolidus assemblage is phlogopite + clinopyroxene ± olivine, the $K_2O$ content in the clinopyroxene increases with increasing temperature. In contrast, at 7.5 GPa, where the assemblage contains garnet, the $K_2O$ content in the clinopyroxene decreases with increasing temperature.

## Melting relationships

The melting of phlogopite + clinopyroxene is incongruent with olivine + clinopyroxene stable with liquid at low pressures and with olivine + clinopyroxene + garnet stable with liquid at higher pressure (Fig. 1). Melting is marked by the disappearance of the hydrous phase phlogopite or amphibole at higher pressure.

The solidus curve extrapolates smoothly from the previous work of Modreski and Boettcher (1973) on the phlogopite-diopside system (Fig. 2). These workers established that the melting of this assemblage was incongruent at 0.5–3 GPa, generating olivine and liquid.

**TABLE 5**—*Extended*

| *P* (GPa) | 11 | 11 | 11 | 14 | 14 | 17 |
|---|---|---|---|---|---|---|
| *T* (°C) | 1300 | 1600 | 1600 | 1300 | 1600 | 1600 |
| Expt. no. | 1107 | 1106 | 1163 | 1105 | 1104 | 1221 |
| *n* | 10 | 6 | 14 | 12 | 4 | 15 |
| $SiO_2$ | 43.8(3) | 45.1(5) | 44.9(3) | 46.4(2) | 48.3(4) | 51.1(6) |
| $Al_2O_3$ | 22.3(6) | 22.0(5) | 21.8(3) | 20.1(6) | 19.3(12) | 11.1(10) |
| MgO | 22.5(6) | 25.4(4) | 25.0(3) | 28.4(10) | 29.7(18) | 27.1(10) |
| CaO | 9.5(9) | 6.5(6) | 7.7(5) | 3.1(13) | 3.9(21) | 10.8(8) |
| $K_2O$ | 0.11(5) | 0.03(1) | 0.05(5) | 0.3(1) | 0.1(1) | 0.2(1) |
| Total | 98.2(2) | 99.1(4) | 99.5(4) | 98.4(3) | 101.3(5) | 100.3(6) |
| | | | **Cations per 12 O atoms** | | | |
| Si | 3.08(2) | 3.11(3) | 3.10(2) | 3.20(2) | 3.24(5) | 3.53(5) |
| Al | 1.85(4) | 1.79(4) | 1.77(2) | 1.63(4) | 1.52(8) | 0.90(8) |
| Mg | 2.36(6) | 2.61(4) | 2.57(4) | 2.92(9) | 3.0(2) | 2.8(1) |
| Ca | 0.72(7) | 0.48(4) | 0.57(3) | 0.2(1) | 0.3(2) | 0.80(6) |
| K | 0.010(5) | 0.002(1) | 0.004(5) | 0.026(8) | 0.005(5) | 0.018(5) |
| Total cations | 8.00(1) | 8.00(1) | 8.018(8) | 8.001(8) | 8.01(2) | 8.03(2) |

**TABLE 6.** Compositions of liquids

| | | | | | | | | |
|---|---|---|---|---|---|---|---|---|
| *P* (GPa) | 5 | 5 | 7.5 | 7.5 | 9 | 9 | 11 | 11 |
| *T* (°C) | 1400 | 1500 | 1450 | 1550 | 1500 | 1550 | 1600 | 1600 |
| Expt. no. | 1179 | 1178 | 1208 | 1213 | 1212 | 1211 | 1106 | 1163 |
| *n* | 11 | 6 | 4 | 4 | 4 | 4 | 3 | 8 |
| $SiO_2$ | 49.7(10) | 49.7(27) | 44.8(18) | 48.6(15) | 45.9(16) | 53.8(2) | 51.4(20) | 45.8(37) |
| $Al_2O_3$ | 11.8(8) | 12.8(12) | 10.8(8) | 7.2(5) | 12.0(23) | 2.5(1) | 3.8(2) | 4.1(11) |
| MgO | 15.5(12) | 15.5(35) | 23.5(16) | 19.7(16) | 22.9(35) | 23.3(1) | 21.0(20) | 21.4(21) |
| CaO | 7.9(13) | 6.2(35) | 1.3(13) | 8.4(30) | 2.3(14) | 7.2(1) | 7.5(31) | 9.6(20) |
| $K_2O$ | 10.3(13) | 11.1(27) | 11.1(6) | 6.9(10) | 10.2(17) | 10.1(2) | 5.2(15) | 7.2(13) |
| Total | 95.2(7) | 95.3(11) | 91.5(19) | 90.8(31) | 93.2(32) | 97.0(2) | 88.9(48) | 88.0(62) |
| | | | | **Estimated melt percentage (wt%)** | | | | |
| From Δtotal | 45 | 46 | 25 | 23 | 32 | 71 | 19 | 18 |
| From modal min | 46 | 43 | 42 | 62 | 45 | 43 | 54 | 66 |

*Note:* *n* = number of analyses. Standard deviations in the last digit(s) are given in parentheses.

Modreski and Boettcher report the composition of quenched liquid from their experiment at 1.5 GPa, 1250 °C on this join. This composition is compared to the higher-pressure results from this study in Figure 3. All of the liquids generated are rich in $SiO_2$ and $K_2O$. The most striking change in the liquid composition with pressure is a distinct increase in the concentration of MgO up to 7.5 GPa. At $P \geq 7.5$ GPa, the melts have ~50 wt% $SiO_2$, ~25 wt% MgO, ~10–15 wt% $K_2O$ and $Al_2O_3$, and low (<5 wt%) CaO. In a broad sense, these liquids are similar to Group II kimberlites and some lamproites (e.g., Mitchell and Bergman 1991). Given the absence of Fe, Ti, and $CO_2$ in the present study, however, further comparison of these liquids with natural rocks is premature.

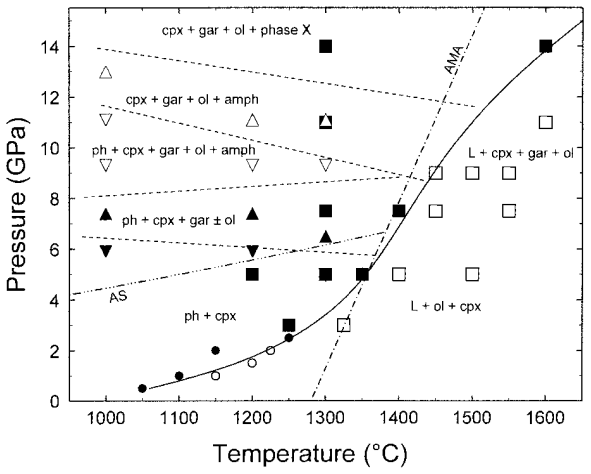


**FIGURE 2.** Pressure-temperature projection of experimental results from this study (squares), from Modreski and Boettcher (1973) (circles; solid symbols are subsolidus experiments; open symbols are supersolidus experiments), and from Sudo and Tatsumi (1990) (triangles: different symbols refer to the different phase assemblages as labeled on the figure). Stable phase assemblages are noted on the diagram, and the inferred boundaries between the differing subsolidus assemblages are drawn as dashed lines. The solidus is shown as a heavy solid line. Also shown on this diagram is the average modern mantle adiabat (AMA, dot-dash line) and a geotherm for an Archean shield (AS, dot-dot-dot-dash line), both from McKenzie and Bickle (1988).

The partitioning of K between clinopyroxene and liquid shows some systematic trends with both temperature (Fig. 4) and pressure (Fig. 5). The value of $D_{K2O}^{cpx/liq}$(wt% $K_2O^{cpx}$/wt% $K_2O^{liq}$) decreases with increasing temperature at 5 GPa, where the phase assemblage is clinopyroxene + olivine + liquid, but increases with increasing temperature at both 7.5 and 9 GPa, where the coexisting phase assemblage includes garnet in addition to olivine and liquid (Fig. 4). This difference illustrates the dependence of the partitioning behavior of K on the phase assemblage present and its effect on the composition of both the liquid and the clinopyroxene. In contrast, the value of $D_{K2O}^{cpx/liq}$ increases systematically with increasing pressure (Fig. 5). Comparison of the partitioning data in this study may be made with the partitioning behavior between clinopyroxene and melt in a lamproitic bulk composition (Edgar and Vukadinovic 1993). Their $D_{K2O}^{cpx/liq}$ values de-

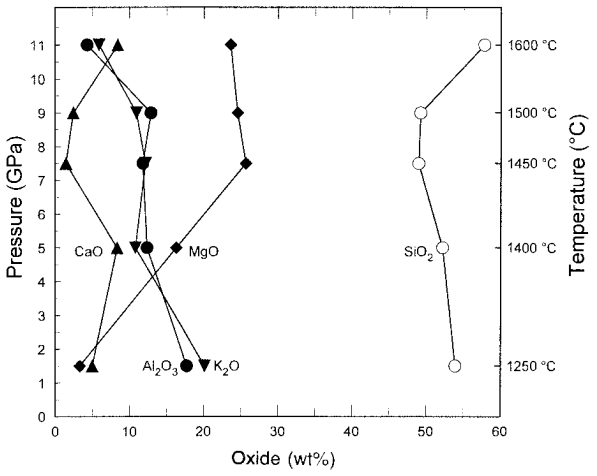


**FIGURE 3.** Compositions of liquids, represented as oxide weight percentages, as a function of pressure. The right-hand ordinate gives the temperature for each experiment. The composition of the lowest-temperature liquid, for a given pressure, is plotted in this figure. The 1.5 GPa liquid data are from Modreski and Boettcher (1973), the other data are from this study. In all cases, the liquid compositions were normalized volatile-free before plotting.

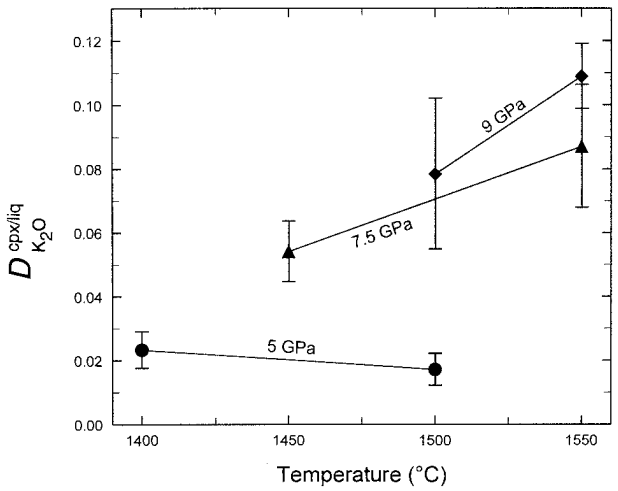


**FIGURE 4.** Partitioning behavior of K between clinopyroxene and liquid as a function of temperature at 5 GPa (circles), 7.5 GPa (triangles), and 9 GPa (diamonds). $D_K^{cpx/liq}$ is defined as (wt% $K_2O^{cpx}$)/(wt% $K_2O^{liq}$). Error bars are ± 1 standard deviation.

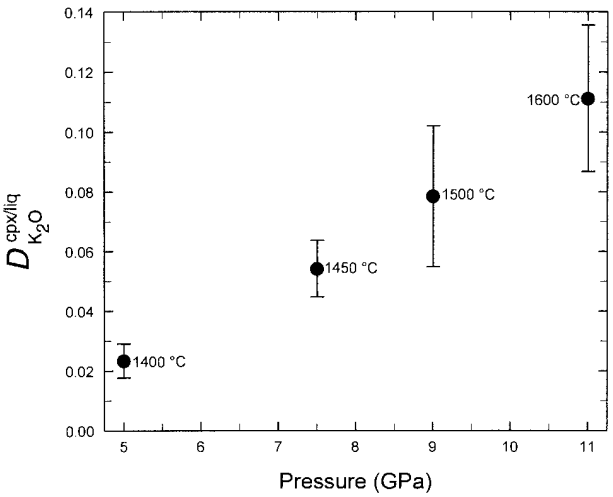


**FIGURE 5.** Partitioning behavior of K between clinopyroxene and liquid as a function of pressure. Temperatures of each experiment are given next to each datum. $D_K^{cpx/liq}$ is defined as (wt% $K_2O^{cpx}$)/(wt% $K_2O^{liq}$). Error bars are ± 1 standard deviation.

crease from 0.195 at 1200 °C to 0.014 at 1450 °C at 5 GPa. The value of 0.023(6) at 5 GPa, 1400 °C from the present study lies on the trend defined by the data of Edgar and Vukadinovic (1993). The slight decrease in $D_{K2O}^{cpx/liq}$ from 1400 ° to 1500 °C observed in the present study may be consistent with the decreasing change in D with increasing temperature observed by Edgar and Vukadinovic (1993). It is possible, based on the agreement between the two sets of data, that the partitioning behavior of K between clinopyroxene and liquid is not sensitive to melt composition, at least over this range of compositions. In both cases, the melts contained 50–60 wt% $SiO_2$ (calculated on an anhydrous basis), and contained ~10 wt% $K_2O$.

The values of $D_{K2O}^{cpx/liq}$ for clinopyroxene and a carbonate-rich liquid are between 0.022 and 0.096 for a variety of bulk compositions (Harlow 1997). These results are consistent with the present study in the sense that both document the marked preference of K for liquid rather than clinopyroxene.

The present melting phase equilibria results may be compared with data for more complex systems previously studied. Lloyd et al. (1985) studied the melting phase relations of a phlogopite-clinopyroxenite nodule at 2 and 3 GPa. In their three GPa experiments, phlogopite + clinopyroxene + ilmenite ± apatite coexist with liquid from 1225 to 1275 °C. At higher temperatures, clinopyroxene alone coexists with the melt. At 2 GPa, the assemblage clinopyroxene + olivine + phlogopite + magnetite + liquid was present at 1200 °C, clinopyroxene + olivine + phlogopite + liquid at 1225 °C, and clinopyroxene + olivine + liquid at 1250 and 1300 °C. The significant difference between these results and those of the present study is the persistence of phlogopite coexisting with melt over a finite temperature interval in the experiments of Lloyd et al. (1985). This persistence probably results from the presence of Fe in their system; the phlogopites in the three GPa experiments are progressively more magnesian with increasing temperature, from Mg/(Mg + Fe) = 0.71 at 1225 °C to 0.84 at 1275 °C.

In a study of the near-liquidus phase relations of a mafic minette, Esperança and Holloway (1987) found that phlogopite and clinopyroxene coexist with liquid over a ~50 °C interval. Again, the micas in their experiments become progressively more magnesian with increasing temperature (Esperança and Holloway 1987, their Table 3).

Sweeney et al. (1993) studied the phase relationships of a natural MARID xenolith from 2 to 3.5 GPa. They found that the melting reactions were phlogopite + clinopyroxene + olivine → phlogopite + clinopyroxene + olivine + liquid at < 3 GPa and phlogopite + clinopyroxene + orthopyroxene → phlogopite + clinopyroxene + olivine + liquid at ≥ 3 GPa. The phlogopite in their experiments also show an increasing Mg/(Mg + Fe) with increasing temperature. All three of these experimental studies document the added complexity of the solid solution behavior of natural micas and the influence of this behavior on the phase relationships in Fe-bearing systems.

### Phase X

An unknown K-rich phase was found at 11 GPa and 1600 °C and at higher pressures. It is of interest because of its high thermal stability, which makes it a potential host for K and $H_2O$ at normal mantle temperatures at these pressures. This phase has variable chemistry (cf. Table 4) but is high in $K_2O$ (10–15 wt%) and MgO (26–30 wt%) and low in $Al_2O_3$. The phase contains ~16 cations per 22 O atoms. This phase may be related to those reported by Trønnes (1990), Harlow (1995), and Inoue et al. (1995). The formula re-

ported by Trønnes (1990) [$K_{3.3}Mg_{6.5}Al_{0.5}Si_{7.0}O_{22}(OH)_2$] translates to a similar composition (in wt%, $K_2O$ 17.6, MgO 29.7, $Al_2O_3$ 2.9, $SiO_2$ 47.7, and $H_2O$ 2.0). Harlow (1995) reports a magnesian montdorite mica of composition $K_2Mg_5Si_8O_{20}$-$[Cl_2(OH)_2]$ in experiments at 8 to 11 GPa, 1350–1450 °C on diopside + talc + KCl. Inoue et al. (1995) report finding an ''X'' phase formed by the decomposition of K-rich amphibole. They found this phase had a molar K:Mg/Si of approximately 1:2/2, and reported a SIMS measurement of 1.69 wt% $H_2O$. More work is needed to characterize this phase and to evaluate its potential to host and transport $H_2O$ in the Earth's mantle.

### Implications for the Earth

Although the simplicity of this system prohibits direct application to the Earth, several consequences emerge that do apply. Clinopyroxene that coexists with phlogopite or the higher-pressure K-rich phases potassium richterite or phase X will have relatively low (~1 wt%) $K_2O$ in them. Conversely, natural clinopyroxenes with higher K concentrations must have formed in environments that lack these more K-rich phases. Another K-rich phase, $KAlSi_3O_8$ hollandite, is stable in K-rich anhydrous assemblages at high pressure, such as subducted terrigenous sediments (Irifune et al. 1994), and may have a similar effect in maintaining a lower K content in coexisting clinopyroxene, but this possibility remains to be evaluated experimentally.

Comparing the experimental results with models of the mantle geotherm [Fig. 2, AMA = average (present-day) mantle adiabat from McKenzie and Bickle 1988], the hydrous phases are stable at mantle temperatures at pressures > 5 GPa. Addition of Fe to the system tends to lower the thermal stability of the hydrous phases. The magnitude of this shift must be calibrated, as must the effect of substitution of F for OH on stabilizing the hydrous phases to higher temperatures. Finally, the character and stability field of phase X await further study.

## Acknowledgments

This research was funded by Research Grants from the National Science and Engineering Research Council of Canada and by Infrastructure and Major Facilities Access Grants from NSERC that support the multiple-anvil laboratory in the C.M. Scarfe Laboratory of Experimental Petrology. Careful and insightful reviews by T. Gasparik and G. Harlow and editorial commentary by D. Jenkins improved the manuscript considerably. G. Harlow is thanked in addition for supplying a preprint of his 1997 paper.

## References cited

Akaogi, M. and Akimoto, S. (1977) Pyroxene-garnet solid-solution equilibria in the systems $Mg_4Si_4O_{12}$-$Mg_3Al_2Si_3O_{12}$ and $Fe_4Si_4O_{12}$-$Fe_3Al_2Si_3O_{12}$ at high pressures and temperatures. Physics of the Earth and Planetary Interiors, 15, 90–106.

Allègre, C.J., Poirier, J.-P., Humler, E., and Hofmann, A.W. (1995) The chemical composition of the Earth. Earth and Planetary Science Letters, 134, 515–526.

Bishop, F.C., Smith, J.V., and Dawson, J.B. (1978) Na, K, P and Ti in garnet, pyroxene and olivine from peridotite and eclogite xenoliths from African kimberlites. Lithos, 11, 155–173.

Boyd, F.R. and Mertzman, S.A. (1987) Composition and structure of the Kaapvaal lithosphere, southern Africa. In B.O. Mysen, Ed., Magmatic Processes: Physicochemical Principles, p. 13–24. Geochemical Society, Special Publication No. 1.

Dawson, J.B. (1980) Kimberlites and their xenoliths, 252 p. Springer-Verlag, Berlin.

Edgar, A.D. and Vukadinovic, D. (1993) Potassium-rich clinopyroxene in the mantle: An experimental investigation of a K-rich lamproite up to 60 kbar. Geochimica et Cosmochimica Acta, 57, 5063–5072.

Erlank, A.J. (1970) Distribution of potassium in mafic and ultramafic nodules. Carnegie Institution of Washington Year Book, 68, 433–439.

Erlank, A.J., Waters, F.G., Hawkesworth, C.J., Haggerty, S.E., Allsopp, H.L., Rickard, R.S., and Menzies, M. (1987) Evidence for mantle metasomatism in peridotite nodules from the Kimberley pipes, South Africa. In M.A. Menzies and C.J. Hawkesworth, Eds., Mantle Metasomatism, p. 221–311. Academic Press, London.

Esperança, S. and Holloway, J.R. (1987) On the origin of some mica-lamprophyres: experimental evidence from a mafic minette. Contributions to Mineralogy and Petrology, 95, 207–216.

Gasparik, T. (1986) Experimental study of subsolidus phase relations and mixing properties of clinopyroxene in the silica-saturated system CaO-MgO-$Al_2O_3$-$SiO_2$. American Mineralogist, 71, 686–693.

———(1993) The role of volatiles in the transition zone. Journal of Geophysical Research, 98, 4287–4299.

Harlow, G.E. (1995) K-amphibole and mica stability in K-rich environments at high P and T. (abstr.) EOS, 76, S298.

———(1996a) CaTs, potassium, and vacancies in aluminous diopside at high pressure. (abstr.) Abstracts with Programs, 28, 1996 Annual Meeting, Geological Society of America, A-47.

———(1996b) Structure refinement of a natural K-rich diopside: The effect of K on the average structure. American Mineralogist, 81, 632–638.

———(1997) K in clinopyroxene at high pressure and temperature: An experimental study. American Mineralogist, 82, 259–269.

Harlow, G.E. and Veblen, D.R. (1991) Potassium in clinopyroxene inclusions from diamonds. Science, 251, 652–655.

Hart, S.R. and Zindler, A. (1986) In search of a bulk-Earth composition. Chemical Geology, 57, 247–267.

Inoue, T. (1994) Effect of water on melting phase relations and melt composition in the system $Mg_2SiO_4$-$MgSiO_3$-$H_2O$ up to 15 GPa. Physics of the Earth and Planetary Interiors, 85, 237–263.

Inoue, T., Irifune, T., Yurimoto, H., and Miyagi, I. (1995) Decomposition of K-amphibole at high pressure: implications for the origin of the third chain volcanism. (abstr.) EOS, 76, F711.

Irifune, T., Ringwood, A.E., and Hibberson, W.O. (1994) Subduction of continental crust and terrigenous and pelagic sediments: an experimental study. Earth and Planetary Science Letters, 126, 351–368.

Kanzaki, M. (1987) Ultrahigh-pressure phase relations in the system $Mg_4Si_4O_{12}$-$Mg_3Al_2Si_3O_{12}$. Physics of the Earth and Planetary Interiors, 49, 168–175.

Kushiro, I. (1970) Stability of amphibole and phlogopite in the upper mantle. Carnegie Institution of Washington Year Book, 68, 245–247.

———(1976) Changes in viscosity and structure of melt of $NaAlSi_2O_6$ composition at high pressures. Journal of Geophysical Research, 81, 6347–6350.

Kushiro, I., Syono, Y., and Akimoto, S. (1967) Stability of phlogopite at high pressures and possible presence of phlogopite in the Earth's upper mantle. Earth and Planetary Science Letters, 3, 197–203.

Liu, L. (1977) The system enstatite-pyrope at high pressures and temperatures and the mineralogy of the Earth's mantle. Earth and Planetary Science Letters, 36, 237–245.

Lloyd, F.E., Arima, M., and Edgar, A.D. (1985) Partial melting of a phlogopite-clinopyroxenite nodule from south-west Uganda: an experimental study bearing on the origin of highly potassic continental rift volcanics. Contributions to Mineralogy and Petrology, 91, 321–329.

Luth, R.W. (1993) Melting in the $Mg_2SiO_4$-$H_2O$ system at 3 to 12 GPa. Geophysical Research Letters, 20, 233–235.

Luth, R.W., Trønnes, R.G., and Canil, D. (1993) Volatile-bearing Phases in the Earth's Mantle. In R.W. Luth, Ed., Short Course Handbook on Experiments at High Pressure and Applications to the Earth's Mantle, p. 445–485. Mineralogical Association of Canada.

McCandless, T.E. and Gurney, J.J. (1989) Sodium in garnet and potassium

in clinopyroxene: criteria for classifying mantle eclogites. In Ross et al., Eds., Kimberlites and Related Rocks, Volume 2. Their mantle/crust setting, diamonds and diamond exploration, p. 827–832. Geological Society of Australia, Special Publication No. 14.

McDonough, W.F. and Sun, S.-S. (1995) The composition of the Earth. Chemical Geology, 120, 223–253.

McKenzie, D. and Bickle, M.J. (1988) The volume and composition of melt generated by extension of the lithosphere. Journal of Petrology, 29, 625–679.

Mitchell, R.H. and Bergman, S.C. (1991) Petrology of lamproites, 447 p. Plenum Press, New York and London.

Modreski, P.J. and Boettcher, A.L. (1972) The stability of phlogopite + enstatite at high pressures: A model for micas in the interior of the Earth. American Journal of Science, 272, 852–869.

———(1973) Phase relationships of phlogopite in the system $K_2O$-MgO-CaO-$Al_2O_3$-$SiO_2$-$H_2O$ to 35 kilobars: A better model for micas in the interior of the Earth. American Journal of Science, 273, 385–414.

Nixon, P.H. and Boyd, F.R. (1973) Petrogenesis of the granular and sheared ultrabasic nodule suite in kimberlites. In P.H. Nixon, Ed., Lesotho kimberlites, p. 48–56. Lesotho National Development Corporation, Maseru.

Plank, T. and Langmuir, C.H. (1993) Tracing trace elements from sediment input to volcanic output at subduction zones. Nature, 362, 739–743.

Reid, A.M., Brown, R.W., Dawson, J.B., Whitfield, G.G., and Siebert, J.C. (1976) Garnet and pyroxene compositions in some diamondiferous eclogites. Contributions to Mineralogy and Petrology, 58, 203–220.

Ringwood, A.E. (1967) Pyroxene-garnet transformations in the Earth's mantle. Earth and Planetary Science Letters, 2, 255–263.

———(1979) Origin of the Earth and Moon, 295 p. Springer-Verlag, New York.

Robert, J-L., Hardy, M., and Sanz, J. (1995) Excess protons in synthetic micas with tetrahedrally coordinated divalent cations. European Journal of Mineralogy, 7, 457–461.

Rosenbaum, J.M. (1993) Mantle phlogopite: a significant lead repository? Chemical Geology (Isotope Geoscience Section) 106, 475–483.

Smith, D.C. (1984) Coesite in clinopyroxene in the Caledonides and its implications for geodynamics. Nature, 310, 641–644.

———(1988) A review of the peculiar mineralogy of the ''Norwegian Coesite-Eclogite Province'', with crystal-chemical, petrological, geochemical and geodynamical notes and an extensive bibliography. In D.C. Smith, Ed., Eclogites and eclogite-facies rocks, p. 1–206. Elsevier, Amsterdam.

Smyth, J.R. (1980) Cation vacancies and the crystal chemistry of breakdown reactions in kimberlitic omphacites. American Mineralogist, 65, 1185–1191.

Smyth, J.R., Caporuscio, F.A., and McCormick, T.C. (1989) Mantle eclogites: evidence of igneous fractionation in the mantle. Earth and Planetary Science Letters, 93, 133–141.

Sudo, A. and Tatsumi, Y. (1990) Phlogopite and K-amphibole in the upper mantle: Implication for magma genesis in subduction zones. Geophysical Research Letters, 17, 29–32.

Sweeney, R.J., Thompson, A.B., and Ulmer, P. (1993) Phase relations of a natural MARID composition and implications for MARID genesis, lithospheric melting and mantle metasomatism. Contributions to Mineralogy and Petrology, 115, 225–241.

Thompson, A.B. and Connolly, J.A.D. (1995) Melting of the continental crust: Some thermal and petrological constraints on anatexis in continental collision zones and other tectonic settings. Journal of Geophysical Research, 100, 15565–15579.

Trønnes, R.G. (1990) Low-Al, high-K amphiboles in subducted lithosphere from 200 to 400 km depth: experimental evidence. (abstr.) EOS, 71, 1587.

von Huene, R. and Scholl, D.W. (1991) Observations at convergent margins concerning sediment subduction, subduction erosion, and the growth of continental crust. Reviews of Geophysics, 29, 279–316.

Walter, M.J., Thibault, Y., Wei, K., and Luth, R.W. (1995) Characterizing experimental pressure and temperature conditions in multianvil apparatus. Canadian Journal of Physics, 73, 273–286.

Waters, F.G. (1987) Suggested origin of MARID xenoliths in kimberlites by high pressure crystallization of an ultrapotassic rock such as lamproite. Contributions to Mineralogy and Petrology, 95, 523–533.

Wood, B.J. and Henderson, C.M.B. (1978) Compositions and unit-cell parameters of synthetic non-stoichiometric tschermakitic clinopyroxenes. American Mineralogist, 63, 66–72.

Yasuda, A., Fujii, T., and Kurita, K. (1994) Melting phase relations of an anhydrous mid-ocean ridge basalt from 3 to 20 GPa: Implications for the behavior of subducted oceanic crust in the mantle. Journal of Geophysical Research, 99, 9401–9414.

Yoder, H.S., Jr. and Kushiro, I. (1969) Melting of a hydrous phase: phlogopite. American Journal of Science, 267-A, 558–582.

Manuscript received October 8, 1996
Manuscript accepted July 2, 1997